

Proceedings for "Organic Photorefractive  
Materials VI" Session of 45<sup>th</sup> SPIE (The Intl. Soc.  
for Optical Engineering), San Diego, CA,  
July 30 - Aug. 4, 2000

ANL/CHM/CP-102579  
RECEIVED  
SEP 12 2000  
OSTI

## Photorefractivity in Ferroelectric Liquid Crystals

Gary P. Wiederrecht<sup>a</sup>, Michael R. Wasielewski<sup>b</sup>, and Michael Fuller<sup>b</sup>,

<sup>a</sup>Chemistry Division, Argonne National Laboratory, Argonne, IL 60439-4831

<sup>b</sup>Department of Chemistry, Northwestern University, Evanston, IL 60208-3113

### ABSTRACT

The first observation of photorefractivity in ferroelectric liquid crystals (flcs) is reported. The flcs are doped with the easily oxidized chromophore perylene, which also functions as the sensitizer. The electron acceptor di-butylpyromellitimide is added to induce photoconductivity through an efficient intermolecular electron transfer reaction to produce mobile ions. A strong dependence on the orientation of the wavevector of the optical interference pattern and polarization of the writing beams relative to the orientation of the flc molecules is observed. The results are interpreted as an orientational photorefractive effect in which the net polarization of the flc couples linearly to the space-charge field as opposed to nematic liquid crystals in which the dielectric anisotropy couples to the square of the space charge field.

**Keywords:** Photorefractive Materials; Ferroelectric Liquid Crystals; Non-Linear Optics; Photoconductivity

### 1. INTRODUCTION

The photorefractive effect is a result of photoinduced charge generation, followed by migration of the more mobile charged species into the non-illuminated region of photoconductive material.<sup>1,2</sup> This effect is usually induced by crossing two coherent laser beams in an electro-optic sample to create an interference pattern of light and dark regions. If a charge trapping mechanism is present, then a long-lived and modulated space-charge field between the light and dark regions of the sample is formed. In fluid materials, the spatial charge distribution is the result of the difference in the diffusion coefficients of the positive and negative charge carriers. In either case, an electro-optic mechanism must be present, either from an orientational response to the space charge field or a second order nonlinear effect in a non-centrosymmetric material. Through these effects, the index of refraction of the material is modulated. This modulated index grating, a nonlocal phase grating, is the result of the photorefractive effect.

Traditional photorefractive materials are inorganic ferroelectric crystals, such as LiNbO<sub>3</sub> or BaTiO<sub>3</sub>.<sup>1,3</sup> These materials possess polar symmetry that induce directional charge transport and lack a center of symmetry so that the electro-optic effect can exist. More recently, organic polymers,<sup>2,4-7</sup> glasses,<sup>8</sup> organic crystals,<sup>9</sup> and liquid crystals<sup>10-18</sup> have been shown to illustrate orientational and/or linear electro-optic photorefractive effects. Composites containing different materials, such as polymers and liquid crystals to form polymer-dispersed, polymer-stabilized, or high molecular weight nematic liquid crystals, have improved the grating resolution of these materials.<sup>15,19-22</sup> These studies are proving liquid crystals to be a versatile addition to the rapidly expanding field of organic photorefractive materials.

Noticeably absent in the literature on new organic photorefractive liquid crystals are ferroelectric liquid crystals (flcs).<sup>23</sup> Appropriately aligned flcs have a net polarization ( $P_s$ ) in the smectic C\* phase and also have a C<sub>2</sub> symmetry that permits, in principle, the observation of second order, electronic electro-optic effects.<sup>24,25</sup> Thus, these materials are fundamentally different than nematic liquid crystals because they have the potential to illustrate photorefractive effects of electronic electro-optic origin, and also orientational effects that are not derived solely from quadratic coupling of the space-charge field to the dielectric anisotropy ( $\Delta\epsilon$ ). In other words, the orientational dynamics in nematics are dominated by the  $\Delta\epsilon E_{sc}^2$  proportionality, but orientational dynamics in flcs are dominated by a polarization term given by  $P_s E_{sc}$ .<sup>26</sup> This linear coupling to the space-charge field is a potentially far stronger orientational effect than is possible in nematic liquid crystals.

We present here the first observation of photorefractivity in flcs. The flc used is a eutectic mixture, CS-1015, commercially available from Chisso Corporation, Japan. The components of the mixture are not supplied, but flcs generally consist of rodlike aromatic molecules with a chiral center. CS-1015 has a phase transition diagram of:

Isotropic  $\rightarrow$  Nematic\*  $\rightarrow$  Smectic A  $\rightarrow$  Smectic C\* (flc)  $\rightarrow$  Crystalline

The submitted manuscript has been created by the University of Chicago as Operator of Argonne National Laboratory ("Argonne") under Contract No. W-31-109-ENG-38 with the U.S. Department of Energy. The U.S. Government retains for itself, and others acting on its behalf, a paid-up, nonexclusive, irrevocable worldwide license in said article to reproduce, prepare derivative works, distribute copies to the public, and perform publicly and display publicly, by or on behalf of the Government.

## **DISCLAIMER**

**This report was prepared as an account of work sponsored by an agency of the United States Government. Neither the United States Government nor any agency thereof, nor any of their employees, make any warranty, express or implied, or assumes any legal liability or responsibility for the accuracy, completeness, or usefulness of any information, apparatus, product, or process disclosed, or represents that its use would not infringe privately owned rights. Reference herein to any specific commercial product, process, or service by trade name, trademark, manufacturer, or otherwise does not necessarily constitute or imply its endorsement, recommendation, or favoring by the United States Government or any agency thereof. The views and opinions of authors expressed herein do not necessarily state or reflect those of the United States Government or any agency thereof.**

## **DISCLAIMER**

**Portions of this document may be illegible in electronic image products. Images are produced from the best available original document.**

CS-1015 has a polarization of  $-6.6 \text{ nC/cm}^2$  and an index of refraction anisotropy of  $\Delta n = 0.14$ . In order to obtain aligned films of fics, we used commercially available cells (Displaytech) with a  $4 \mu\text{m}$  spacing that have a rubbed polyimide layer that are designed to align fics. The liquid crystal was placed at the edge of the cell in the isotropic phase at  $90^\circ\text{C}$  and drawn into the cell through capillary action. The cell was then slowly cooled at  $0.5^\circ\text{C/hr}$  to room temperature.

The fic aligns in a manner contingent upon the spacer thickness and the pitch length of the fic. The different alignment possibilities are a result of the well known helical pattern of fics, in which the polarization of the molecules rotates in a helical pattern with a pitch length typically on the order of a few microns.<sup>24,27</sup> The two most common alignment options are illustrated in Figure 1 for: a) spacer thickness greater than the pitch length and b) spacer thickness less than the pitch length. The glass slides lie in the plane of the page for this figure. For the first option, a homogeneously aligned fic will possess a precessing director ( $n$ ) perpendicular to the planes of the  $\text{Sm C}^*$  liquid crystal. This produces a rotating spontaneous polarization ( $P_s$ ) and no macroscopic polarization. However, at a relatively low applied field ( $\sim 1\text{V}/\mu\text{m}$ ), the helix can be unwound and the molecular dipoles can align with the field, as shown in Figure 1a.<sup>28</sup> This produces the "bookshelf" geometry, where the long axes of the molecules are aligned parallel to the plane of the glass slides, with a tilt angle  $\theta$  off of the rubbing axis. The molecular dipole is oriented perpendicular to the long axis and points toward the face of the cell. This orientation produces macroscopic polarization in the material. When the opposite polarity electric field is applied, the dipole switches orientation and produces a rotation of the long axis by  $2\theta$ , as illustrated in Figure 1. This change in birefringence produces the on/off states between crossed polarizers for which fics are known, with the optimal value for  $\theta = 22.5^\circ$ .<sup>29</sup>

The second alignment option, shown in Figure 1b, is the surface stabilized fic (SSFLC), which results when the pitch length is greater than the spacer thickness.<sup>24</sup> This configuration is bistable, meaning that only a short voltage pulse of  $\sim 10\text{V}/\mu\text{m}$  is required to switch the polarization direction. Furthermore, the fic orientation is maintained in the absence of any applied electric field.

## 2. EXPERIMENTAL METHODS

We did not see evidence of bistability in the absence of an applied field, indicating that the CS-1015 composite is not aligned in the SSFLC state. This is consistent with the short pitch length for CS-1015 of  $3 \mu\text{m}$  and the  $4 \mu\text{m}$  spacer thickness, so that a helical orientation of the fic is produced. When an applied field of magnitude  $\sim 1 \text{ V}/\mu\text{m}$  was used, the unwound helix configuration was achieved as evidenced by the extinction/transmission of light through cross polarizers with a rotation of the cell by  $2\theta$  of  $45^\circ$ , in reasonable agreement with the supplier's data on this fic of  $2\theta = 52^\circ$ . An additional factor that may contribute to the lack of bistability is the presence of ions, which are known to adversely influence bistable states.<sup>30</sup>

The experimental apparatus is illustrated in Figure 2. We use an  $\text{Ar}^+$  laser at  $514 \text{ nm}$  that is split into two beams of  $15 \text{ mW}$  each. The beams are overlapped at an angle  $\theta' = 8^\circ$  at the sample to create an optical interference pattern with  $\Lambda = 2.1 \mu\text{m}$ . An applied voltage of up to  $22\text{V}$  is used, producing an applied field  $E_A$  up to  $5.5 \text{ V}/\mu\text{m}$ . The sample is tilted relative to the bisector of the beams by  $\beta = 32.5^\circ$ . This induces directional charge transport along the wavevector of the optical interference pattern, so that spatial modulation of the charge distribution is possible, as illustrated in Figure 2. The inset

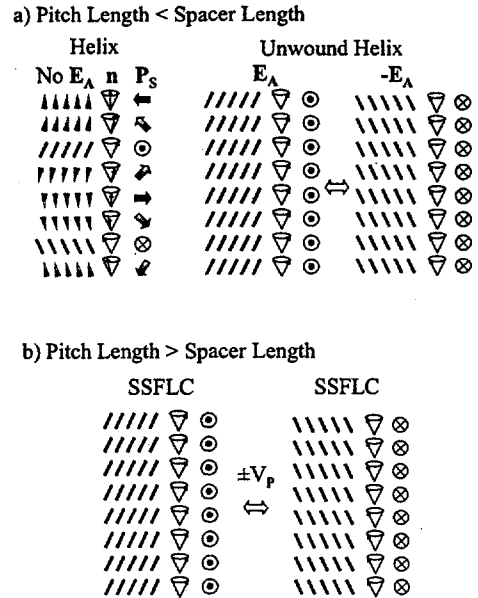


Figure 1. Two alignment possibilities for fics are illustrated. For these illustrations, the glass slides are parallel to the page. a) The pitch length is less than the spacer thickness, leading to a helical orientation of the polarization in the absence of an applied field. When a field is applied, the helix is unwound, leading to a net polarization. The molecular orientation can be switched by switching the polarity of the applied field. b) The pitch length is greater than the spacer thickness, leading to a surface stabilized fic. No applied field is necessary to maintain alignment of the polarization and only a voltage pulse is required to switch the molecular orientation.

illustrates the optical interference and the relative orientation of the flc molecules in an applied field, for the applied field normal to the plane of the page. The angle  $\phi$  is the rotation angle used to maximize beam coupling. Finally, the writing beams are s-polarized, i.e. perpendicular to the wavevector, and no photorefractive beam-coupling was observed for p-polarized beams. This contrasts with the observation that only p-polarized beams lead to beam coupling in homeotropically aligned liquid crystals.<sup>10,12,13</sup> Finally, no beam coupling was observed in the absence of an applied field or without tilting the cell relative to the bisector of the writing beams.

The values for  $\Lambda = 2.1$  and  $4 \mu\text{m}$  cell thickness produce a quality value ( $Q$ ), a measure of the degree of Bragg character of the grating, of  $\sim 2$ . Since  $Q$  values of  $\sim 10$  are required to produce true Bragg gratings, this grating possesses a degree of Raman-Nath (thin grating) character.<sup>31</sup> In the thin grating regime, the use of a photorefractive gain coefficient ( $I \propto e^{-\Gamma d}$ , where  $I$  is intensity,  $\Gamma$  is the gain coefficient, and  $d$  is the optical path length) on thickness has been debated, with some groups reporting an exponential gain coefficient.<sup>14,32,33</sup> We choose here to report only a beam coupling ratio, i.e.  $I_{12}/I_1$  where  $I_{12}$  is the intensity of beam one in the presence of beam 2 and  $I_1$  is the intensity of beam 1 in the absence of beam two.

The dopant molecules are chosen to provide for a small amount of absorption at the laser wavelength and to produce photoinduced charge separation.<sup>34</sup> The first dopant is perylene (PER), which functions as both the sensitizer and the electron donor in a photoinduced, intermolecular charge transfer reaction. The second dopant is dibutyl pyromellitimide (PI), an easily reduced molecule that has no visible absorption.<sup>35</sup> These dopants have been used in nematic liquid crystals and this combination has an optimal free energy for charge separation to produce mobile ions in liquid crystals.<sup>34</sup> The concentration of PER =  $2 \times 10^{-3}$  M and PI =  $4 \times 10^{-3}$  M. This produces an absorption coefficient of  $\alpha \sim 1 \text{ cm}^{-1}$ . The photoconductivity ( $\sigma_{ph}$ ) of the cell with 22 V applied is  $4.5 \times 10^{-12} \Omega^{-1} \cdot \text{cm}^{-1}$  and the dark conductivity is  $9 \times 10^{-13} \Omega^{-1} \cdot \text{cm}^{-1}$ .

### 3. RESULTS

The conductivity and nonlinear optical effects should be highly anisotropic, so that the relative orientation of the smectic planes and molecular orientations relative to the wavevector of the optical interference pattern should produce changes in the photorefractive beam coupling ratio. Figure 3 illustrates the beam coupling ratio as a function of the rotation  $\phi$  of the cell. Also illustrated is the transmission of one of the beams through cross polarizers, so that the relative orientation of the molecules relative to the wavevector can be determined. At  $0^\circ$  and  $180^\circ$ , the smectic planes and the wavevector of the optical interference pattern are parallel. The orientation of the molecules is illustrated between the two graphs for the applied field  $E_A$  at which the beam coupling is measured and the second row of orientations is for the opposite polarity  $-E_A$ . Since the polarization of the writing beams is perpendicular to the wavevector, the maximum extinction, i.e. when the molecular orientation is parallel to the polarization of the writing beams, is at  $\phi = 20^\circ$  or  $200^\circ$ .

Figure 3 illustrates a spike in the beam coupling ratio at  $\phi = 100^\circ$  and a smaller spike at  $\phi = 240^\circ$ . For most of the rotation angles  $\phi$ , no significant beam coupling is observed. Figure 4 schematically illustrates the orientation of the flc and the regions where photorefractivity is observed. In the region around  $100^\circ$  where maximum beam coupling is observed, the molecules are oriented with their long axis nearly perpendicular to the polarization of the writing beams and parallel to the wavevector of the grating. This provides some clues as to the electrooptic mechanism and the space charge field buildup. First, for this orientation, charge migration along the wavevector is approximately parallel to the flc director.  $E_{SC}$  has the following space charge field dependence:

$$E_{SC} = \frac{-k_B T K (D^+ - D^-) \sigma_{ph}}{2\epsilon_0 (D^+ + D^-) (\sigma_{ph} + \sigma_d)} \sin Kx \quad (1)$$

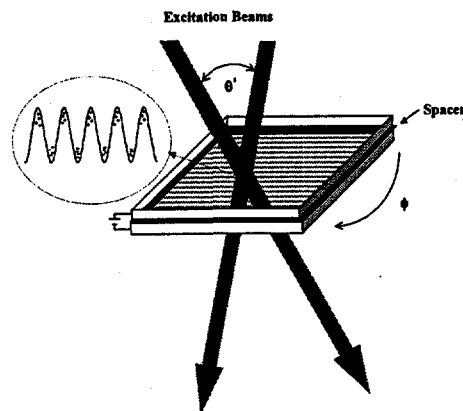
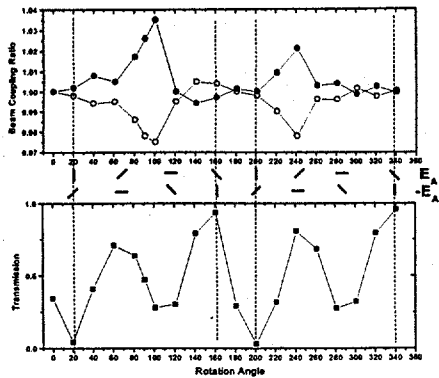
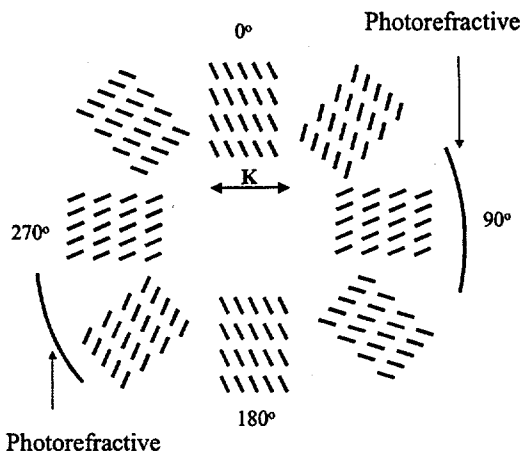


Figure 2. A schematic of the experimental geometry is illustrated. The sample is tilted at an angle  $\beta = 32.5^\circ$  relative to the bisector of the two beams. This allows for charge migration along the grating wavevector which results in a sinusoidal space charge field. The beams are polarized perpendicular to the grating wavevector. The planes of the smectic C\* flc can be rotated by an angle  $\phi$  relative to the wavevector direction.



**Figure 3.** The dependence of beam coupling ratio on the rotation angle  $\phi$  is shown. Also shown is the transmission through cross polarizers of a vertically polarized beam for an applied field  $E_A$  at which beam coupling ratio is observed compared to the transmission at  $-E_A$ . The relative orientations of the molecules are shown for  $E_A$  and  $-E_A$ .



**Figure 4.** A schematic of the orientation of the flc as a function of rotation angle  $\phi$ , along with the regions where photorefractivity is observed is shown.

Here,  $\sigma_{ph}$  is the photoconductivity,  $\sigma_d$  is the dark conductivity,  $k_B$  is the Boltzmann constant,  $K$  is the grating wavevector,  $x$  is the direction along the wavevector,  $e_0$  is the charge of the electron, and  $D^+$  and  $D^-$  are the diffusion constants for the cations and anions, respectively. This equation assumes that the intensities of the two incident beams are equal ( $I_1=I_2$ ). It is clear that the two factors which determine the magnitude of the space charge field are the difference in the photoconductivity versus dark conductivity and the difference in the diffusion coefficients of the cations and anions. It should also be noted that previous experimental results have shown that ion transport in flcs is such that only one charge carrier is mobile, supporting the ability of flcs to possess a spatially modulated charge density.<sup>36</sup> The diffusion of the more mobile species is maximized at this orientation, with ions moving approximately parallel to the long molecular axis.

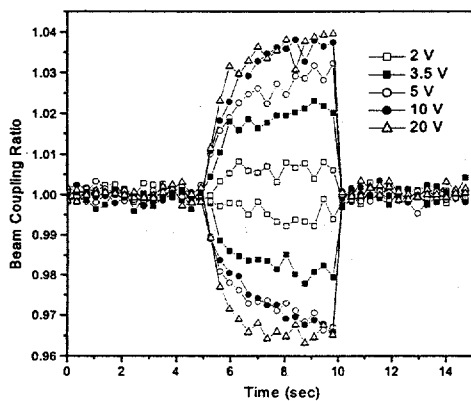


**Figure 5.** The dependence of the beam coupling ratio on applied voltage is illustrated.

In the present flc composite, the photorefractive electro-optic mechanism is derived from orientational effects and not the linear electrooptic effect. First, the majority of flcs have a small degree of electronic second-order nonlinear character, as measured by small electro-optic coefficients ( $r_{ij}$ ) that are 1-2 orders of magnitude lower than their crystalline counterparts.<sup>37</sup> The few exceptions are flcs that utilize molecules with large hyperpolarizabilities aligned along the polar axis.<sup>25,37,38</sup> Second, the  $r_{22}$  coefficient dominates the electronic electrooptic mechanism in flcs. In this tilted geometry, accessing  $r_{22}$  would require the writing beams to be p-polarized where no photorefractivity is observed. The s-polarized beams are consistent with an orientational response, because the maximum signal is obtained when the molecules are aligned nearly perpendicular to the light polarization. In this region, an angular change of the molecular orientation produces the largest change in the index of refraction as a component of the long axis begins to align with the light polarization.

Although orientational photorefractivity is still dominant in flcs as with nematics, the mechanism for orientational coupling to the space-charge field is different. As stated above, the reorientation of the molecules in flcs can occur through a coupling to the polarization, i.e. proportional to  $PE_{SC}$ , as opposed to nematic materials in which the reorientation is coupled solely to the dielectric anisotropy ( $\Delta\epsilon$ ), proportional to  $\Delta\epsilon E_{SC}^2$ . Figure 5 shows the dependence of the beam coupling ratio on applied voltage, which is far less than the  $(V_A E_{SC})^2$  dependence of diffraction efficiency previously shown for nematics, where  $V_A$  is the applied voltage.<sup>10</sup> The beam coupling ratio in the flc composite is saturated for an applied voltage of 10V, but larger applied voltages give a faster grating formation time.

For a nematic material, a  $180^\circ$  rotation should lead to equivalent birefringent contributions. However, for a flc, the two orientations lead to opposite displacement directions around the conical axis shown in Figure 1. This can lead to different changes in the birefringence due to  $E_{SC}$  and a different value for the beam coupling ratio. We believe that this may be the reason for the reduced beam coupling centered at  $\phi = 240^\circ$ . It should be noted that no photorefractivity was observed in three other flcs (CS-1014, CS-1022, and CS-1028). The clear difference between CS-1015 and the other flcs is a lower orientational viscosity for CS-1015 of  $211 \text{ mPa} \cdot \text{s}$  vs 280, 349, and  $325 \text{ mPa} \cdot \text{s}$  for flcs CS-1014, CS-1022, and CS-1028, respectively. This observation is probably the result of increased orientational birefringence and/or increased mobilities of ions in this environment.

The reorientational capabilities of the flc director in response to a switch in the polarity of the applied field could lead to novel possibilities for on/off switching of the photorefractive effect. Since we have shown that the photorefractive effect in flcs is strongly correlated with the alignment of the flc molecules relative to the writing beam polarization, a reorientation of the molecules in response to a polarity switch in the applied field could act to quickly increase or decrease the beam coupling ratio in flc composites. Figure 6 shows the beam coupling changes for an orientation of  $100^\circ$ , where photorefractivity is maximized for an applied voltage of 20V. At 10 s, the voltage is switched to  $-20\text{V}$  for 5 s. The signal is corrected for a small change in the transmission (not through cross polarizers) when the polarity switch occurs. A rapid decrease in the beam coupling is observed, consistent with a molecular reorientation of  $45^\circ$  to a region where less photorefractivity is observed. This is followed by a slower erasure of the modulated space-charge field as charges begin to redistribute in response to the applied field polarity change. At 20 s, the voltage is switched back to 20V, and the initial charge modulation begins to reform.

#### 4. CONCLUSIONS

We have observed for the first time orientational photorefractivity in flc composites containing easily oxidized and reduced chromophores. The applied field dependence suggests that the orientational response is a result of the space charge field coupling to the bulk polarization of the flc and not to dielectric anisotropy as with nematic liquid crystals. It should be possible to rapidly improve this effect in flcs. One possibility is to use homeotropically aligned flcs with a transverse applied field, so that the modulated space charge field lies along the polar axis of the flc. This would increase the likelihood of observing the linear electronic electro-optic effect in addition to orientational contributions. The use of flcs specifically designed for increasing  $P_S$  and the linear electro-optic effect would also be helpful. With these improvements, significant improvements to these materials should be possible.

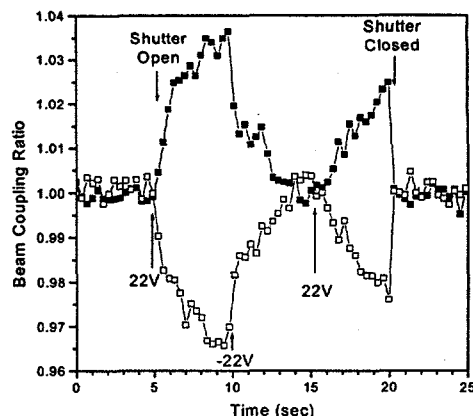


**Figure 6.** The change of the beam coupling ratio when the applied voltage is switched from 22V to  $-22\text{V}$  is shown. The rapid initial decrease is due to the reorientation of the flc director to a less optimal orientation for photorefractivity. The slower change is due to the erasure of the space charge field.

## 5. ACKNOWLEDGMENTS

The authors gratefully acknowledge support from the Office of Naval Research under Grant No. N00014-99-1-0411 (MRW) and the Office of Advanced Scientific Computing Research, Technology Research Division, DOE under contract W-31-109-ENG-38 (GPW). GPW also acknowledges support from DOE for the Presidential Early Career Award for Scientists and Engineers.

## 6. REFERENCES

- 1)Gunter, P.; Huignard, J. P. *Photorefractive Materials and Their Applications 1: Fundamental Phenomena*; Springer-Verlag: Berlin, 1988.
- 2)Moerner, W. E.; Grunnet-Jepsen, A.; Thompson, C. L. *Annu. Rev. Mater. Sci.* **1997**, *27*, 585-623.
- 3)Ashkin, A.; Boyd, G. D.; Dziedzic, J. M.; Smith, R. G.; Ballman, A. A.; Lexinstein, J. J.; Nassau, K. *Appl. Phys. Lett.* **1966**, *9*, 72.
- 4)Ducharme, S.; Scott, J. C.; Twieg, R. J.; Moerner, W. E. *Phys. Rev. Lett.* **1991**, *66*, 1846-1849.
- 5)Meerholz, K.; Volodin, B. L.; Sandalphon; Kippelen, B.; Peyghambarian, N. *Nature* **1994**, *371*, 497-500.
- 6)Yu, L.; Chan, W. K.; Peng, A.; Gharavi, A. *Acc. Chem. Res.* **1996**, *29*, 13-21.
- 7)Winiarz, J. G.; Zhang, L.; Lal, M.; Friend, C. S.; Prasad, P. N. *J. Am. Chem. Soc.* **1999**, *121*, 5287-95.
- 8)Lundquist, P. M.; Wortmann, R.; Geletneky, C.; Twieg, R. J.; Jurich, M.; Lee, V. Y.; Moylan, C. R.; Burland, D. M. *Science* **1996**, *274*, 1182-85.
- 9)Sutter, K.; Hulliger, J.; Schlessler, R.; Gunter, P. *Opt. Lett.* **1993**, *18*, 778-80.
- 10)Khoo, I. C.; Li, H.; Liang, Y. *Opt. Lett.* **1994**, *19*, 1723-25.
- 11)Khoo, I. C. *IEEE J. Quant. Elec.* **1996**, *32*, 525-534.
- 12)Rudenko, E. V.; Sukhov, A. V. *JETP Lett.* **1994**, *59*, 142-46.
- 13)Rudenko, E. V.; Sukhov, A. V. *JETP* **1994**, *78*, 875-882.
- 14)Wiederrecht, G. P.; Yoon, B. A.; Wasielewski, M. R. *Science* **1995**, *270*, 1794-97.
- 15)Ono, H.; Saito, I.; Kawatsuki, N. *Appl. Phys. Lett.* **1998**, *72*, 1942-44.
- 16)Bartkiewicz, S.; Miniewicz, A.; Kajzar, F.; Zagorska, M. *Appl. Opt.* **1998**, *37*, 6871-6877.
- 17)Cipparrone, G.; Mazzulla, A.; Simoni, F. *Opt. Lett.* **1998**, *23*, 1505.
- 18)Tabiryian, N. V.; Umeton, C. *J. Opt. Soc. Am. B* **1998**, *15*, 1912-17.
- 19)Golemme, A.; Volodin, B. L.; Kippelen, B.; Peyghambarian, N. *Opt. Lett.* **1997**, *22*, 1226-28.
- 20)Ono, H. *Opt. Lett.* **1997**, *22*, 1144-46.
- 21)Wiederrecht, G. P.; Wasielewski, M. R. *J. Am. Chem. Soc.* **1998**, *120*, 3231-3236.
- 22)Zhang, J.; Singer, K. D. *Appl. Phys. Lett.* **1998**, *72*, 2948-2950.
- 23)Meyer, R. B.; Liebert, L.; Strzelecki, L.; Keller, P. *J. Phys. Lett.* **1975**, *36*, 69.
- 24)Clark, N. A.; Lagerwall, S. T. *Appl. Phys. Lett.* **1980**, *36*, 899.
- 25)Liu, J.-Y.; Robinson, M. G.; Johnson, K. M.; Walba, D. M.; Ros, M. B.; Clark, N. A.; Shao, R.; Doroski, D. *J. Appl. Phys.* **1991**, *70*, 3426-30.
- 26)Khoo, I. C. *Liquid Crystals: Physical Properties and Nonlinear Optical Phenomena*; Wiley: New York, 1995.
- 27)Cuculescu, I.; Alexe-Ionescu, A. L.; Bena, R.; Ghizdeanu, C.; Stoian, V.; Barbero, G.; Ionescu, A. T. *Mod. Phys. Lett. B* **1995**, *9*, 791-799.
- 28)Ostrowschi, B. I.; Rabinovich, A. Z.; Chigrinov, V. G.; Bata, L., Ed.; Pergamon press: Oxford, 1980.
- 29)Escher, C.; Wingen, R. *Adv. Mater.* **1992**, *4*, 189-97.
- 30)Yang, K. H.; Chieu, T. C.; Osofsky, S. *Appl. Phys. Lett.* **1989**, *55*, 125-7.
- 31)Eichler, H. J.; Gunter, P.; Pohl, D. W. *Laser-Induced Dynamic Gratings*; Springer-Verlag: Berlin, 1986.
- 32)Nolte, D. D.; Olson, D. H.; Doran, G. E.; Knox, W. W.; Glass, A. M. *J. Opt. Soc. Am. B* **1990**, *7*, 2217-25.
- 33)Khoo, I. C.; Guenther, B. D.; Wood, M. V.; Chen, P.; Shih, M.-Y. *Opt. Lett.* **1997**, *22*, 1229-31.
- 34)Wiederrecht, G. P.; Yoon, B. A.; Wasielewski, M. R. *Adv. Mat.* **1996**, *8*, 535-39.
- 35)Osuka, A.; Yamada, H.; Maruyama, K.; Mataga, N.; Asahi, T.; Ohkouchi, M.; Okada, T.; Yamazaki, I.; Nishimura, Y. *J. Am. Chem. Soc.* **1993**, *115*, 9439-9452.
- 36)Maximus, B.; Ley, E. D.; Meyere, A. D.; Pauwels, H. *Ferroelectrics* **1991**, *121*, 103-112.
- 37)Trollsas, M.; Orrenius, C.; Sahlen, F.; Gedde, U. W.; Norin, T.; Hult, A.; Hermann, D.; Rudquist, P.; Komitov, L.; Lagerwall, S. T.; Lindstrom, J. *J. Am. Chem. Soc.* **1996**, *118*, 8542-8548.

38) Kapiza, H.; Zentel, R.; Twieg, R. J.; Nguyen, C.; Vallerien, S. U.; Kremer, F.; Willson, C. G. *Adv. Mater.* 1990, 11, 539-43.